Directed Self-Assembly of Functionalized Silica Nanoparticles on Molecular Printboards through Multivalent Supramolecular Interactions

Venkataramanan Mahalingam,† Steffen Onclin, Mária Péter, Bart Jan Ravoo, Jurriaan Huskens,* and David N. Reinhoudt*

Laboratory for Supramolecular Chemistry and Technology, MESA+ Institute for Nanotechnology, University of Twente, P.O. Box 217, 7500 AE Enschede, The Netherlands

Received August 12, 2004. In Final Form: September 22, 2004

Silica nanoparticles functionalized with β-cyclodextrin (CD) host molecules (**5**) have been prepared by reacting carboxylic active ester-terminated silica nanoparticles (**4**) with CD heptamine. Silica nanoparticles functionalized with glucosamine (**6**), having similar surface properties as **5** but lacking the host−guest recognition motif, were used to perform blank experiments. The CD-functionalized silica nanoparticles **5** were determined by TEM to be 55 ± 6 nm in size. They exhibited pH-dependent aggregation, which is explained by the presence of free amino and carboxylic acid groups on the particle surface, which was corroborated by zeta potential measurements. The functionalization with CD was further confirmed by host−guest studies in solution and at CD-functionalized silicon substrates. The addition of an adamantyl-terminated dendrimer, capable of multivalent host−guest binding with CD, led to strong aggregation of the CD particles **5**, but not of the glucosamine-functionalized **6**. Furthermore, **5** gave strong adsorption to CD monolayers on silicon onto which adamantyl-terminated dendrimers were adsorbed, whereas **6** did not. The good discrimination between dendrimer-covered and uncovered areas of the CD monolayer substrates allowed the directed self-assembly of the silica particles **5** onto dendrimer-patterned areas created by microcontact printing.

Introduction

Particles ranging in size typically from 1 nm to several μm play a major role in the development of nanoscience and nanotechnology. Nanoparticles are promising candidates for the construction of new nanomaterials.[1,2] These nanostructured materials possess interesting structures and are expected to have great significance in designing devices for sensors[3] and single molecule detectors.[4] The controlled organization and precise positioning of nanoparticles on 2D surfaces for the fabrication of 3D nanoscale colloidal architectures are essential for the development of novel materials such as photonic band gap (PBG) materials,[5−9] optoelectronic devices,[10−13] composites,[14] and so forth. The electronic, optical, and sensor applications of nanoparticle arrays on surfaces have been reviewed by Shipway et al.[15] Various techniques such as electrostatic assembly,[16−18] convective self-assembly,[19,20] physisorption mediated by surface tension,[21,22] colloidal epitaxy,[23] and application of an external electric field[24] have been employed to direct the assembly of nanoparticles on surfaces. Capillary[25,26] and entropic[27] forces have also been utilized for the self-organization of nanoparticles on 2D surfaces.

Among the various techniques mentioned above, electrostatic self-assembly has been most widely used to direct nanoparticle assembly on surfaces. This method can easily be extended to grow multilayers by alternate deposition of oppositely charged polyions. This method is well known as layer-by-layer (LBL) assembly as first introduced by Decher.[28] Hammond's group has exploited this approach to grow multilayers with polystyrene and silica nanoparticles.[29−31] They have also demonstrated the use of this

* Authors to whom correspondence should be addressed. E-mail: j.huskens@utwente.nl; E-mail: d.n.reinhoudt@utwente.nl.
† Present address: University of Victoria, Canada.

(1) Fendler, J. H. *Nanoparticles and Nanostructured Films: Preparation, Characterization and Applications;* Wiley-VCH: Weinheim, Germany, 1998.
(2) Shimomura, M.; Sawadaishi, T. *Curr. Opinion Colloid Interface Sci*. **2001**, *6*, 11.
(3) Wohltjen, H.; Snow, A. W. *Anal. Chem*. **1998**, *70*, 2856.
(4) Nie, S.; Emory, S. R. *Science* **1997**, *275*, 1102.
(5) Yang, S. M.; Ozin, G. A. *Chem. Commun*. **2000**, 2057.
(6) Gates, B.; Xia, Y. *Adv. Mater*. **2000**, *12*, 1329.
(7) Xia, Y.; Gates, B.; Yin, Y.; Lu, Y. *Adv. Mater*. **2000**, *12*, 693.
(8) Xia, Y.; Gates, B.; Park, S. H. *J. Lightwave Technol*. **1999**, *17*, 1956.
(9) Park, S. H.; Xia, Y. *Langmuir* **1998**, *15*, 266.
(10) Yang, P.; Wirnsberger, G.; Huang, H. C.; Cordero, S. R.; McGehee, M. D.; Scott, B.; Deng, T.; Whitesides, G. M.; Chmelka, B. F.; Buratto, S. K.; Stucky, G. D. *Science* **2000**, *287*, 465.
(11) Hattori, H. *Adv. Mater*. **2001**, *13*, 51.
(12) Deutsch, M.; Vlasov, Y. A.; Norris, D. J. *Adv. Mater*. **2000**, *12*, 1176.
(13) Joannopoulos, J. D.; Villeneuve, P. R.; Fan, S. H. *Nature* **1997**, *386*, 143.
(14) Rao, M. P.; Sanchez-Herencia, A. J.; Beltz, G. E.; McMeeking, R. M.; Lange, F. F. *Science* **1999**, *286*, 102.
(15) Shipway, A. N.; Katz, E.; Willner, I. *ChemPhysChem*. **2000**, *1*, 18.
(16) Schmitt, J.; Machtle, P.; Eck, D.; Mohwald, H.; Helm, C. A. *Langmuir* **1999**, *15*, 3256.
(17) Tien, J.; Terfort, A.; Whitesides, G. M. *Langmuir* **1997**, *13*, 5349.
(18) Auer, F.; Scotti, M.; Ulman, A.; Jordan, R.; Selergren, B.; Garno, J.; Liu, G.-Y. *Langmuir* **2000**, *16*, 7554.
(19) Jiang, P.; Bertone, J. F.; Hwang, K. S.; Colvin, V. L. *Chem. Mater*. **1999**, *11*, 2132.
(20) Jiang, P.; Ostojic, G. N.; Narat, R.; Mittleman, D. M.; Colvin, V. L. *Adv. Mater*. **2001**, *13*, 389.
(21) Lenzmann, F.; Li, K.; Kitai, A. H.; Stover, H. D. H. *Chem. Mater*. **1994**, *6*, 156.
(22) Deckman, H. W.; Dunsmuir, J. H.; Gruner, S. M. *J. Vac. Sci. Technol., B* **1989**, *7*, 1832.
(23) Van Blaaderen, A.; Wiltzius, P. *Adv. Mater*. **1997**, *9*, 833.
(24) Yeh, S.-R.; Seul, M.; Shraiman, B. I. *Nature* **1997**, *386*, 57.
(25) Aizenberg, J.; Braun, P. V.; Wiltzius, P. *Phys. Rev. Lett*. **2000**, *84*, 2997.
(26) Yin, Y.; Gates, B.; Xia, Y. *J. Am. Chem. Soc*. **2001**, *123*, 8718.
(27) Hutchinson, T. O.; Liu, Y.-P.; Kiely, C.; Kiely, C. J.; Brust, M. *Adv. Mater*. **2001**, *13*, 1800.
(28) Decher, G. *Science* **1997**, *277*, 1232.
(29) Lee, I.; Zheng, H.; Rubner, M. F.; Hammond, P. T. *Adv. Mater*. **2002**, *14*, 572.

10.1021/la047982w CCC: $27.50
Published on Web 11/12/2004

method to assemble a bicomponent array consisting of two different types of nanoparticles on a prepatterned surface.[32] This method allows the underlying chemical pattern to be intensified by the construction of additional layers of nanoparticles. Furthermore, gold nanoparticle/dendrimer composite materials prepared via LBL assembly display vapor-sensing properties.[33] Covalent interactions have been utilized as well to bind nanoparticles to preferred regions of a substrate.[34,35] Patterning of protein nanostructures has been achieved through the deposition of nanoparticles carrying proteins.[36]

Here, we describe a method to direct nanoparticle assembly by supramolecular host−guest interactions. In principle, this could lead to improved selectivity and ease of assembly as the interactions between particle surface and substrate can be fine-tuned using well-known and well-studied host−guest motifs. Earlier, we reported the use of β-cyclodextrin (CD) monolayers on gold and silicon oxide substrates as molecular printboards for positioning multivalent guest molecules through supramolecular interactions.[37] Recently, we have shown how these molecular printboards can be applied as a platform to create molecular patterns of guest-functionalized calixarene molecules and dendritic wedges labeled with fluorescent groups using microcontact printing and dip-pen nanolithography.[38] A clear target, therefore, is now to apply these molecular printboards for the assembly of nanoparticles since the thermodynamic and kinetic parameters for the assembly of multivalent species are well understood.[39] Here, we describe the preparation of CD-functionalized silica nanoparticles and their host−guest chemistry with multivalent guest-functionalized dendrimers, which leads to aggregation of the CD silica nanoparticles. In addition, the adsorption of CD-functionalized silica nanoparticles onto CD printboards, which are fully or partly (by microcontact printing) modified with guest-functionalized dendrimers, is discussed.

Experimental Section

Chemicals. Tetraethyl orthosilicate, 3-aminopropyl triethoxysilane (APTES), glutaric anhydride, concentrated ammonium hydroxide, *N*′-(3-dimethylaminopropyl)-*N*-ethylcarbodiimide hydrochloride (EDC), *N*-hydroxysuccinimide (NHS), 2-(*N*-morpholino)-ethanesulfonic acid (MES), 4-(2-hydroxyethyl)piperazine-1-ethanesulfonic acid (HEPES), *d*-glucosamine hydrochloride (GA), absolute ethanol (>99.8%), and dimethylformamide (>99.8%) were obtained from commercial sources. Milli-Q water with resistance greater than 18 MΩ was used in all our experiments. β-Cyclodextrin heptamine was synthesized as described before.[40] Generation 1 and 5 adamantyl-terminated poly(propylene imine) (PPI) dendrimers (with 4 and 64 adamantyl groups, respectively) were synthesized as reported before.[41]

Preparation of Buffer Solutions. A standard buffer concentration of 0.1 M in water was used throughout the experiments unless mentioned otherwise. The final pH of the buffers was adjusted with 1 M NaOH or 1 M HCl to the desired pH. Carbonate buffer (pH 9.2) was prepared by mixing 4 mL of 0.1 M sodium carbonate and 46 mL of 0.1 M sodium bicarbonate. HEPES buffer (pH 7.2) was prepared by dissolving 2.38 g of HEPES free acid in 100 mL water and adjustment with NaOH. MES buffer (pH 5.6) was prepared by dissolving 4.8 g of MES free acid in 250 mL water and adjustment with NaOH. Acetate buffer (pH 4.0) was prepared by mixing 41 mL of 0.1 M acetic acid with 9 mL of 0.1 M sodium acetate and diluting to 100 mL (buffer concentration 0.05 M).

Preparation of Bare Silica Nanoparticles (1). The bare silica nanoparticles were synthesized following a literature procedure.[42] Briefly, 3.8 mL of tetraethyl orthosilicate was added to a flask containing 5.7 mL of concentrated ammonium hydroxide and 114 mL of ethanol while stirring. The stirring was continued overnight. This resulted in the formation of approximately 50 nm silica nanoparticles **1**.

Preparation of Amino-Functionalized Silica Nanoparticles (2). Silica nanoparticles **1** were functionalized with APTES by quickly adding 1 mL of APTES to 50 mL of a vigorously stirred dispersion of **1** in ethanol, and the mixture was allowed to stir overnight at room temperature (r.t.). The nanoparticles were purified by centrifugation and redispersion in ethanol, which was repeated three times.

Preparation of Carboxylic Acid-Functionalized Silica Nanoparticles (3). A dispersion of **2** in DMF was prepared by centrifugating a dispersion of **2** in ethanol, redispersing them in ethanol:DMF 1:1, followed by centrifugation and redispersion in DMF. The opaqueness of the colloidal dispersion had decreased once the particles were dispersed in DMF. Ten milliliters of this solution was added dropwise to a flask containing 114 mg (1 mmol) of glutaric anhydride dissolved in 10 mL DMF. The mixture was left to stir overnight. The excess glutaric anhydride was removed by centrifugation and redispersion of the particles in DMF, which was repeated twice. The silica nanoparticles **3** were finally redispersed in water by slowly increasing the ratio of H_2O/DMF. The increase in the H_2O/DMF ratio was accompanied by an increase in the opaqueness of the colloidal dispersion.

Preparation of NHS Ester-Functionalized Silica Nanoparticles (4). The carboxylic acid groups of silica nanoparticles **3** were activated with EDC and NHS by adding 5 mL of a dispersion of **3** in MES buffer to a flask containing a mixture of 10 mM of EDC and NHS. After 1 h stirring, the particles were centrifuged and redispersed in carbonate buffer to give the NHS ester-terminated silica nanoparticles **4**.

Preparation of β-Cyclodextrin-Functionalized Silica Nanoparticles (5). A dispersion of **4** in carbonate buffer (5 mL) was added dropwise to a flask containing 5 mL of 10 mM β-cyclodextrin heptamine while stirring. Stirring was continued for another 3 h at r.t. The excess of β-cyclodextrin heptamine was removed by centrifugation and redispersion of the silica nanoparticles, which was repeated three times. Finally, the silica nanoparticles **5** were redispersed in carbonate buffer and stored at 4 °C. For all pH dependent studies, the silica nanoparticles in carbonate buffer were centrifuged and redispersed in the corresponding buffer solutions.

Preparation of Glucosamine-Functionalized Silica Nanoparticles (6). A dispersion of **4** in carbonate buffer (5 mL) was added dropwise to a flask containing 5 mL of 10 mM glucosamine in carbonate buffer while stirring. Stirring was continued for another 3 h at r.t. The excess of glucosamine was removed by centrifugation and redispersion of the silica nanoparticles, which was repeated three times. Finally, the silica nanoparticles **6** were redispersed in carbonate buffer and stored at 4 °C. For all pH dependent studies, the silica nanoparticles in carbonate buffer were centrifuged and redispersed in the corresponding buffer solutions.

(30) Chen, K. M.; Jiang, X.; Kimerling, L. C.; Hammond, P. T. *Langmuir* **2000**, *16*, 7825.
(31) Hammond, P. T. *Curr. Opin. Colloid Interface Sci*. **2000**, *4*, 430.
(32) Zheng, H.; Lee, I.; Rubner, M. F.; Hammond, P. T. *Adv. Mater.* **2002**, *14*, 569.
(33) Krasteva, N.; Besnard, I.; Guse, B.; Bauer, R. E.; Mullen, K.; Yasuda, A.; Vossmeyer, T. *Nano Lett*. **2002**, *2*, 551.
(34) Jonas, U.; del Campo, A.; Krüger, C.; Glasser, G.; Boos, D. *Proc. Natl. Acad. Sci. U.S.A.* **2002**, *99*, 5034.
(35) Himmelhaus, M.; Takei, H. *Phys. Chem. Chem. Phys*. **2002**, *4*, 496.
(36) Gleason, N. J.; Nodes, C. J.; Higham, E. M.; Guckert, N.; Aksay, I. A.; Schwarzbauer, J. E.; Carbeck, J. D. *Langmuir* **2003**, *19*, 513.
(37) Huskens, J.; Deij, M. A.; Reinhoudt, D. N. *Angew. Chem., Int. Ed*. **2002**, *41*, 4467.
(38) Auletta, T.; Dordi, B.; Mulder, A.; Sartori, A.; Onclin, S.; Bruinink, C. M.; Péter, M.; Nijhuis, C. A.; Beijleveld, H.; Schönherr, H.; Vancso, G. J.; Casnati, A.; Ungaro, R.; Ravoo, B. J.; Huskens, J.; Reinhoudt, D. N. *Angew. Chem., Int. Ed*. **2004**, *43*, 369.
(39) Huskens, J.; Mulder, A.; Auletta, T.; Nijhuis, C. A.; Ludden, M. J. W.; Reinhoudt, D. N. *J. Am. Chem. Soc.* **2004**, *126*, 6784.
(40) Guillo, F.; Jullien, L.; Hamelin, B.; Lehn, J.-M.; De Robertis, L.; Driguez, H. *Bull. Soc. Chim. Fr*. **1995**, *132*, 857.
(41) Baars, M. W. P. L.; Karlsson, A.; Sorokin, V.; De Waal, B. F. M.; Meijer, E. W. *Angew. Chem., Int. Ed.* **2000**, *39*, 4262.
(42) Hiramatsu, H.; Osterloh, F. E. *Langmuir* **2003**, *19*, 7003.

Table 1. Average Hydrodynamic Radius of β-Cyclodextrin- (5) and Glucosamine- (6) Functionalized Silica Nanoparticles in Different Buffer Solutions

pH (buffer)	r_{av} of **5** (nm)	r_{av} of **6** (nm)
9.2 (carbonate)	115	95
7.2 (HEPES)	>1000	95
5.6 (MES)	>1000	94
4.0 (acetate)	690	136

Transmission Electron Microscopy (TEM). TEM images were collected on a Philips CM 30 Twin STEM fitted Kevex delta plus X-ray dispersive electron spectroscopy (EDX) and Gatan model 666 PEELs operating at 300 kV. Samples for imaging were deposited onto a 200 mesh copper grid and left to dry for 5 min.

Dynamic Light Scattering (DLS). The DLS experiments were performed with a Zetasizer 4000 (Malvern Instruments Ltd., U.K.) at 25 °C using a laser wavelength of 633 nm at a scattering angle of 90°. Results obtained are the averages of three measurements. The average hydrodynamic radius (r_{av}) of β-cyclodextrin- (**5**) and glucosamine- (**6**) functionalized silica nanoparticles at various pH values was determined on 1 mL samples of **5** or **6** in the corresponding buffer solutions (Table 1). The (attempted) aggregation of **5** and **6** with the G1 adamantyl-terminated PPI dendrimer was performed by measuring r_{av} for a 1 or 0.5 mL sample (for **5** and **6**, respectively) and after subsequent additions of 25, 50, 100, and 200 μL of a 25 μM solution of the G1 dendrimer. The dispersions were gently shaken before the measurements for proper mixing.

Zeta Potentials. Zeta potentials of the silica nanoparticles **3**, **5**, and **6** were obtained with a Zetasizer 2000 (Malvern Instruments Ltd., U.K.) using the Laser Doppler velocimetry technique in which the velocity of the particles in a fluid that results from an applied electric field is measured. Measurements were performed at 25 °C using a 1000 Hz modulator frequency and a cell drive voltage of 120 V. The values reported are the averages of three measurements.

Preparation of β-Cyclodextrin Printboards on Silicon Oxide. The β-cyclodextrin monolayers on the native oxide of silicon wafers were prepared using a previously published four-step procedure.[43] Briefly, a cyano-terminated monolayer was formed by exposing an oxidized silicon substrate to a solution of 1-trichlorosilyl-11-cyanoundecane in toluene. After removal of the excess silane, the cyano-terminated monolayers were reduced by Red Al in toluene. Subsequently, the amine-terminated monolayer was reacted with phenylene diisothiocyanate in toluene to obtain isothiocyanate-terminated monolayers. These were reacted with β-cyclodextrin heptamine in water to obtain the β-cyclodextrin monolayers. All monolayer substrates were characterized with contact angle measurements, ellipsometry, Brewster-angle FTIR, and XPS.[43]

Silica Nanoparticles on β-Cyclodextrin Printboards on Silicon Oxide. The attachment of β-cyclodextrin- (**5**) and glucosamine- (**6**) functionalized silica nanoparticles to β-cyclodextrin printboards on silicon oxide was tested on bare β-cyclodextrin printboards and on printboards with G5 adamantyl-terminated PPI dendrimers adsorbed onto them. The latter were prepared by dipping the β-cyclodextrin printboards into an aqueous solution (0.1 mM of Ad functionalities) of the G5 adamantyl-terminated PPI dendrimer containing an excess of β-cyclodextrin at pH 2, as reported previously.[37] Particle deposition was performed on the bare and dendrimer-adsorbed printboards by contacting the substrates with a drop of a dispersion **5** or **6** in carbonate buffer for 2 min. β-Cyclodextrin printboards on silicon oxide were patterned by microcontact printing with an aqueous solution (0.1 mM of Ad functionalities) of the G5 adamantyl-terminated PPI dendrimer containing an excess of β-cyclodextrin at pH 2 using a PDMS stamp (with 2-μm-wide lines with a periodicity of 5 μm) hydrophilized with UV/ozone. Hereafter, the patterned substrates were contacted with a drop of a dispersion of the β-cyclodextrin-functionalized silica nanoparticles **5** in carbonate buffer for 2 min. All nanoparticle substrates were washed with copious amounts of carbonate buffer and dried carefully with N_2 to avoid any multilayer formation.[29] A Nanoscope IIIa (Veeco, Digital Instruments) was used to obtain the tapping mode atomic force microscopy (AFM) images. The AFM was equipped with a z scanner. The tips used were made of Si with a nominal spring constant of 37−56 N/m. All images were acquired in air.

Results and Discussion

Scheme 1 illustrates the various steps involved in the preparation of β-cyclodextrin- (CD-) covered silica nanoparticles. Bare silica nanoparticles were prepared using a literature procedure.[42] This method is a slight modification of the well-known Stöber method.[44] The relatively monodisperse silica nanoparticles were generated by the hydrolysis and condensation of tetraethyl orthosilicate in the presence of ammonia as a catalyst. Silica nanoparticles **1** were converted into amino-terminated silica nanoparticles **2** by reaction with 3-aminopropyl triethoxysilane (APTES). The concentration of the silica nanoparticles was estimated to be about 2×10^{12} per mL.[42] The silica nanoparticles **2** were converted into **3** by reaction with glutaric anhydride.[45] The conversion was qualitatively tested by adding salicylaldehyde. Upon addition of salicylaldehyde, **2** turned yellow immediately, indicating the presence of amino groups, whereas a yellow precipitate was hardly observed for **3** even after 24 h. This is a clear indication that most of the amino groups in **3** have reacted. Furthermore, **3** could be easily dispersed in aqueous medium whereas **2** coagulated in water. There was hardly any change in the size of the nanoparticles before and after the conversion as verified with dynamic light scattering (DLS). The carboxylic acid groups of **3** were activated with EDC and NHS to give **4**. The silica nanoparticles **4** were converted into **5** and **6** by reaction with CD heptamine and glucosamine, respectively.

The size distribution of the CD nanoparticles **5** was studied by transmission electron microscopy (TEM). A histogram (Figure 1, bottom) shows the relatively narrow particle size distribution of 55 ± 6 nm. Furthermore, the TEM image (Figure 1, top) shows the absence of aggregation, thus excluding covalent cross-linking between silica nanoparticles by the CD heptamine. Our attempts to use characterization techniques such as IR, XPS, and NMR were not successful in providing details on the binding of CD molecules to the silica particles, mostly because of too few discrimination possibilities between **4** and **5** and severe line broadening.

Indirect evidence for the binding of CD heptamine in **5** comes from the pH-dependent aggregation behavior of these particles in different buffer solutions. The average hydrodynamic radii (r_{av}) obtained from DLS measurements for dispersions of **5** at different pH values are given in Table 1. For comparison, hydrodynamic radii for the glucosamine nanoparticles **6** are also given. The nanoparticle dispersions **5** and **6** are quite monodisperse in carbonate buffer (pH 9.2). At pH 7.2, 5.6, and 4.0, the colloidal dispersions of **5** coagulated as indicated by the (much) larger r_{av} at these pH values, whereas this was not observed for dispersions of **6**. This difference is attributed to the possibly zwitterionic nature of **5**. Nanoparticles **5** may contain both free amino and carboxylic acid groups when it is assumed (i) that not all amino groups of CD heptamine have reacted with active ester groups of **4** and (ii) that not all active ester groups of **4** have reacted with an amino group (or that not all carboxylic

(43) Onclin, S.; Mulder, A.; Huskens, J.; Ravoo, B. J.; Reinhoudt, D. N. *Langmuir* **2004**, *20*, 5460.

(44) Stöber, W.; Fink, A.; Bohn, E. *J. Colloid Interface Sci.* **1968**, *26*, 62.

(45) Levy, L.; Sahoo, Y.; Kim, K.-S.; Bergey, E. J.; Prasad, P. N. *Chem. Mater.* **2002**, *14*, 3715.

Scheme 1. Preparation of β-Cyclodextrin- (5) and Glucosamine- (6) Functionalized Silica Nanoparticles

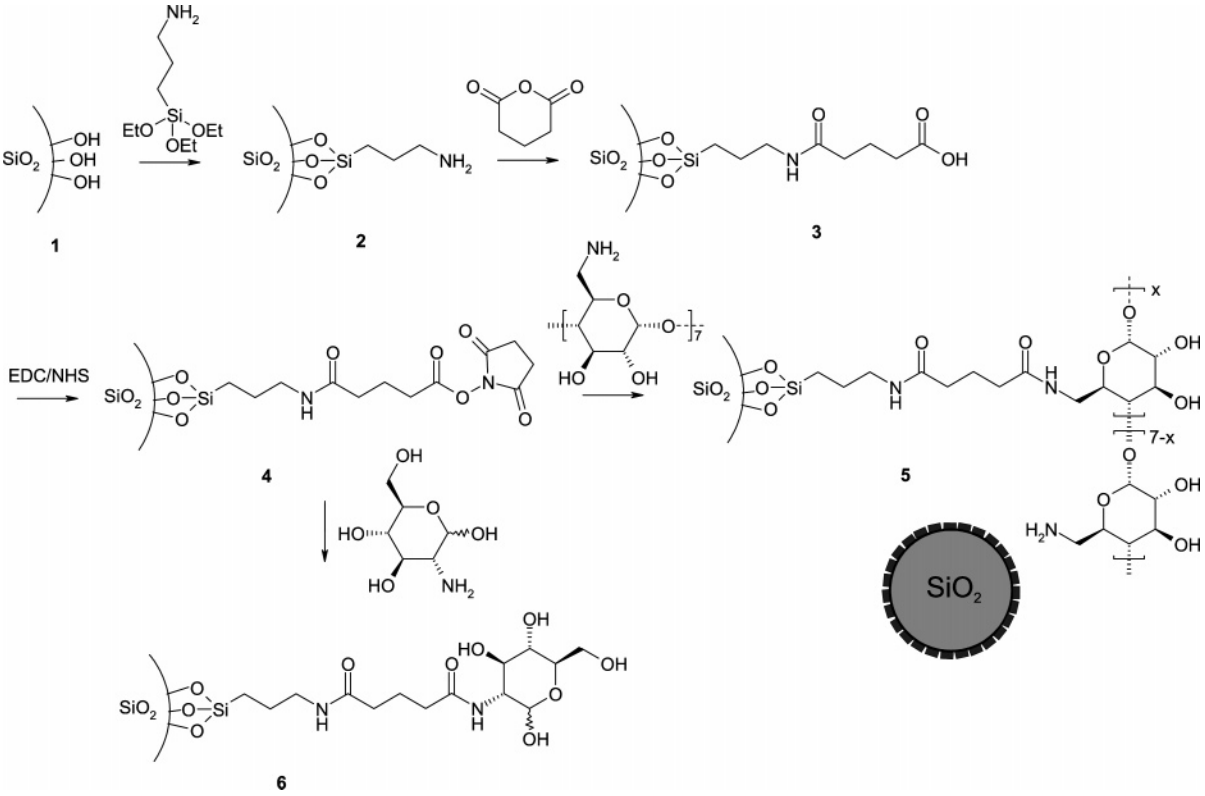

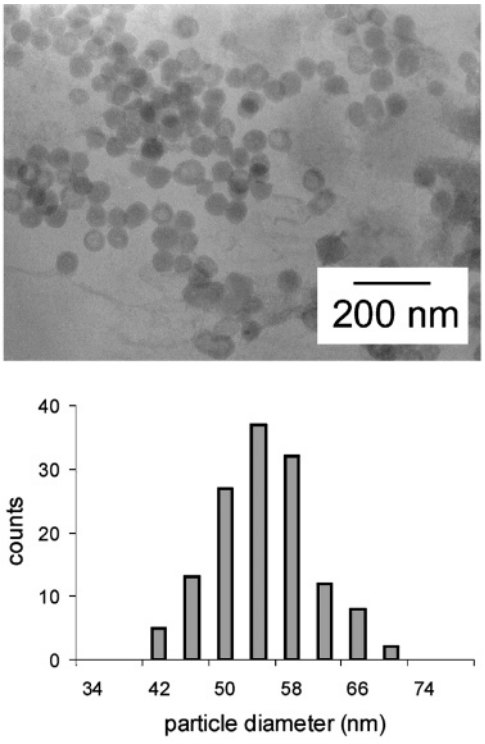

Figure 1. TEM image (top) and histogram (bottom) showing the size distribution of β-cyclodextrin-functionalized silica nanoparticles **5**.

acid groups of **3** have been activated). This would lead to a pH-dependent protonation degree of both the free carboxylic acid and amino groups, causing the existence of an isoelectric point, above and below which the particles are negatively and positively charged, respectively. In contrast, nanoparticles **6** cannot contain free amino groups since the reacting amine is monovalent. Therefore, these are expected to be negatively charged at least as long as part of the unreacted carboxylic acid groups are deprotonated.

The above observations were further substantiated by zeta potential measurements. The zeta potential arises mainly from the presence of surface charges on the nanoparticles.[46] Figure 2 shows a plot of the zeta potentials of

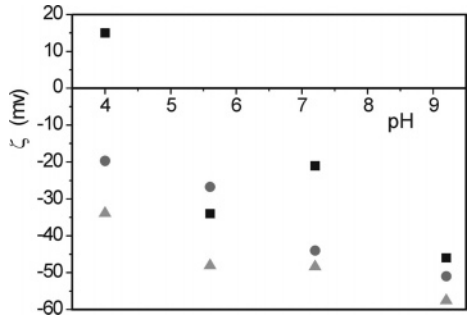

Figure 2. Plot of the zeta potential, ζ, of the functionalized silica nanoparticles **3** (▲), **5** (■), and **6** (●) as a function of the pH of the buffer solution.

3, **5**, and **6** as a function of the pH of the buffer solutions. The large negative values for all three nanoparticle dispersions in carbonate buffer (pH 9.2) reveal the negative charge of these particles at this pH and explain the dispersion stability of these particles at this pH.[46] The highest negative charge is always observed for **3**. As expected, a gradual diminishment of the potential is observed at lower pH values, because of partial protonation of the carboxylate groups. The same effect is observed for **6**, although the absolute values are smaller because of a

(46) (a) Hunter, R. J. *Zeta Potential in Colloid Science*; Academic Press: New York, 1981. (b) Hiemenz, P. C. *Principles of Colloid and Surface Chemistry*; Marcel Dekker: New York, 1977; p 381.

Scheme 2. Schematic Representation of the Aggregation of β-Cyclodextrin-Functionalized Silica Nanoparticles 5 by the Multivalent Host−Guest Interactions with G1 Adamantyl-Terminated PPI Dendrimers

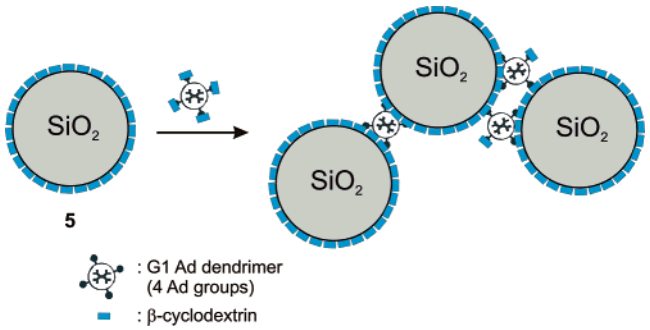

lower surface density of free carboxylate groups because part of them have reacted with glucosamine. Also for **5** this behavior appears to hold at pH 7.2 and 5.6. At pH 4.0, however, the zeta potential of **5** is reversed to positive. This is explained by the protonation of free amino groups concurrent with the protonation of carboxylate groups, leading to charge inversion. From Figure 2 it can be estimated that the isoelectric point of **5** is between pH 4 and 5. The fact that this pH is very close to the pK_a of carboxylic acid groups may indicate that the number of free carboxylic acid groups on **5** is larger than the number of free amino groups. This is plausible since the large size of the CD molecule prevents reaction with all underlying active ester groups at the nanoparticle surface of **4**.[47] The same reasoning holds for **6** so that the fact that particles **6** are strongly negatively charged cannot be taken as a sign of inefficiency of the amide coupling reaction.

The host−guest complexation abilities of **5** in solution were investigated by studying the complexation-induced aggregation of the CD-functionalized silica nanoparticles in the presence of multivalent guest molecules as schematically shown in Scheme 2. This is conceptually similar to, for example, a study of the aggregation of gold nanoparticles induced by avidin−biotin interactions.[48] As the guest molecule, we employed the generation 1 (G1) adamantyl-terminated poly(propylene imine) (PPI) dendrimer, which has four adamantyl groups and the complexation of which with CD[49] and with CD self-assembled monolayers (SAMs) on gold[37] has been described before. Recently, we showed that the analogous ferrocene-terminated dendrimer binds to CD SAMs in a divalent fashion,[39,50] leaving two guest functionalities free for complexation of hosts from solution. Therefore, we viewed this guest molecule ideal for inducing aggregation by the formation of strong, divalent host−guest complexes between two particles. Since the particles are fairly large (53 nm diameter) compared to the dendrimers (about 2 nm),[49] the CD surface can be practically regarded as flat.[51] Because of the multipoint attachment of the CD molecules to the particle surface, the host cavities are pointing with

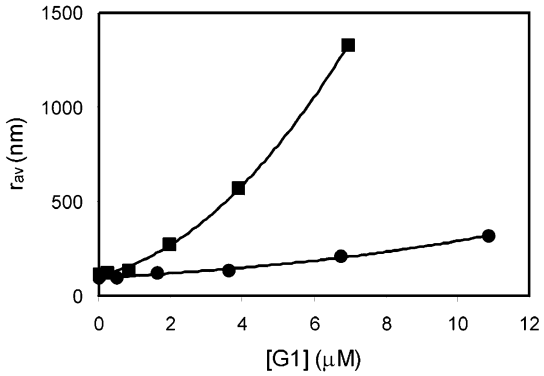

Figure 3. The average hydrodynamic radius, r_{av}, of β-cyclodextrin- (**5**: ■) and glucosamine- (**6**: ●) functionalized silica nanoparticles as a function of the concentration of G1 adamantyl-terminated PPI dendrimer (the parabolic trendlines serve as a guide to the eye only).

their secondary sides to the solution which is ideal for complexation. Thus, the binding behavior of guests to the CD-functionalized nanoparticles is expected to be similar to the CD printboards on silicon oxide which we described recently.[43]

We monitored the change in the average hydrodynamic radius, r_{av}, of the particle dispersions **5** and **6** in carbonate buffer (approximately 2×10^{12} mL^{-1}) with DLS as a function of the concentration of added G1 dendrimer (Figure 3). It is obvious that aggregation is strongly induced for **5**, but barely for **6**. This confirms the specificity of the host−guest interactions in the dendrimer-induced aggregation of **5**. The (much smaller) increase of r_{av} for **6** is probably due to nonspecific hydrophobic or electrostatic interactions. The latter cannot be avoided since the nanoparticles are negatively charged in a carbonate buffer (see above) while the dendrimers are positively charged by partial protonation of the core amines.[49]

The concentration of particle-bound CD cavities in the solution can be estimated from the particle concentration and the number of CDs per particle[51] to be about 10 μM. Since the binding strength of an individual Ad−CD interaction is only about 5×10^4 M^{-1}, aggregation is not expected to occur when the G1 dendrimer would bind in a monovalent fashion only. Thus, the observed aggregation confirms the expected divalent binding mechanism mentioned above. From Figure 3, it can also be seen that the aggregation of **5** starts at [G1] > 1 μM and becomes pronounced at a ratio of guest-bound adamantyl groups to particle-bound CDs of about 1 (which corresponds to [G1] = 2.5 μM). This is plausible when it can be assumed that all adamantyl groups and all particle CD sites can be involved in host−guest binding. Combined with the fact that the dendrimer-particle binding is divalent, this suggests that the surface density of CD sites on the silica nanoparticles is high enough for efficient divalent binding of the G1 dendrimer. Since the adamantyl groups of the G1 dendrimer are spaced just far enough to simultaneously bind to two CD cavities at a molecular printboard,[50] this strongly suggests that the CD surface density at the silica nanoparticles is comparable.

The strong, specific, and multivalent host−guest interactions were employed to bind the CD-functionalized silica nanoparticles to surfaces. We employed the same host−guest chemistry at the substrate as on the nano-

(47) From our work on CD self-assembled monolayers on gold (see Beulen, M. W. J.; Bügler, J.; De Jong, M. R.; Lammerink, B.; Huskens, J.; Schönherr, H.; Vancso, G. J.; Boukamp, B. A.; Wieder, H.; Offenhäuser, A.; Knoll, W.; Van Veggel, F. C. J. M.; Reinhoudt, D. N. *Chem. Eur. J.* **2000**, *6*, 1176), it can be estimated that about 14 alkyl chains fit under a CD cavity suggesting that the ratio between (reacted and unreacted) carboxylic acid and (reacted and unreacted) amino groups is at least 2.

(48) Connolly, S.; Fitzmaurice, D. *Adv. Mater.* **1999**, *11*, 1202.

(49) Michels, J. J.; Baars, M. W. P. L.; Meijer, E. W.; Huskens, J.; Reinhoudt, D. N. *J. Chem. Soc., Perkin Trans. 2* **2000**, 1914.

(50) Nijhuis, C. A.; Huskens, J.; Reinhoudt, D. N. *J. Am. Chem. Soc.* **2004**, *126*, 12266.

(51) When assuming a similar surface density of CD molecules on the nanoparticle surface as on the CD printboards on gold (6×10^{-11} mol cm^{-2}, see ref 39), the number of CD molecules per particle can be estimated to be about 3000.

Scheme 3. Schematic Representation of the Assembly of β-Cyclodextrin-Functionalized Silica Nanoparticles 5 on β-Cyclodextrin Molecular Printboards on Silicon Oxide through Multivalent Host−Guest Interactions Employing the G5 Adamantyl-Terminated PPI Dendrimer as a Supramolecular Glue

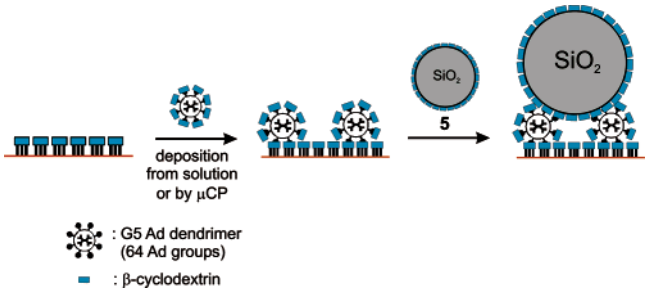

particles. Therefore, we used the CD printboards on silicon oxide, as described before.[43] As a molecular glue between substrate and nanoparticles, we used the G5 adamantyl-terminated PPI dendrimers which contain 64 endgroups because these form kinetically stable complexes at CD monolayers which can be rinsed with large amounts of competitive aqueous solutions without substantial removal.[37,52] The sequential adsorption of the dendrimers and the CD nanoparticles is schematically shown in Scheme 3.

The G5 dendrimer was adsorbed from aqueous solutions as the per-CD complex, as described before.[37] Figures 4a and 4b show AFM images after 2 min adsorption of the CD-functionalized silica nanoparticles **5** on CD printboards on silicon oxide with and without adsorbed G5 dendrimers, respectively. They clearly show that the nanoparticle adsorption is only efficient in the presence of the dendrimer glue. This glue allows the multivalent attachment of the CD silica nanoparticles to the adamantyl groups of the adsorbed G5 dendrimers which remain free for binding after the adsorption to the printboards. According to the AFM height images, a monolayer of particles is obtained, further confirming the specificity of the host−guest interactions and the absence of nonspecific interactions. When the glucosamine-functionalized silica nanoparticles **6** were used on the CD printboards with adsorbed G5 dendrimers (Figure 4c), the coverage was very low, confirming that specific host−guest interactions are needed for efficient adsorption.

The specificity of the CD silica nanoparticles for binding to the dendrimer-covered printboards is high enough to direct the assembly of the nanoparticles to targeted areas on a substrate by prepatterning the substrate with dendrimers. Therefore, we employed microcontact printing[53] to create line patterns of the G5 dendrimers onto which samples the CD silica nanoparticles **5** were adsorbed from solution (see Scheme 3). Figure 4d shows the nearly perfect specificity of the process as the particles formed a densely packed monolayer only in the areas which were contacted with the dendrimer-inked stamp in the preceding step. Thus, it is clear that specific supramolecular interactions can provide an excellent tool to tune the

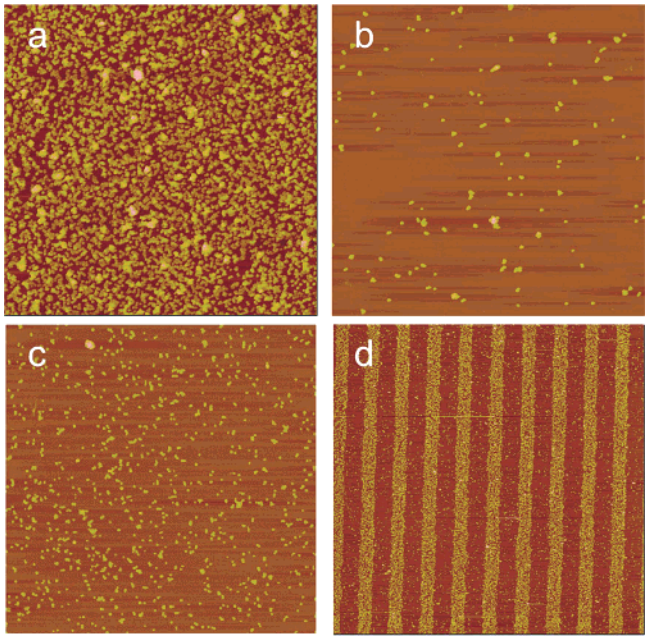

Figure 4. AFM height images (*z* scale: a, b: 250 nm; c, d: 300 nm) obtained after the deposition (2 min at pH 9.2) of β-cyclodextrin- (**5**; a, b, d) and glucosamine-functionalized silica nanoparticles (**6**; c) on β-cyclodextrin printboards on silicon substrates with (a, c) and without (b) the preceding deposition of G5 adamantyl-terminated PPI dendrimers from solution or (d) the microcontact printing of the G5 dendrimers in 2-μm-wide lines; image sizes are 10 × 10 μm^2 and 50 × 50 μm^2 for a−c and d, respectively.

interactions between particles and surfaces and thus to exert control over the formation of 2D nanoparticle patterns.

Conclusions

In conclusion,we have shown that silica nanoparticles can be covalently equipped with host molecules, which allows control over interparticle and particle−surface interactions in water by employing strong, specific, and multivalent host−guest interactions at the interfaces. The CD-functionalized particles behave as noninteracting particles only at a sufficiently high pH where the particles are negatively charged because of the presence of unreacted carboxylate groups at the particle surface. At this pH, aggregation can be induced by the addition of multivalent guest molecules which are able to bridge two particles. This process has been extrapolated to flat surfaces where the same host−guest chemistry allows the strong adhesion of the nanoparticles to the substrates. The specificity is demonstrated by the fact that efficient adsorption is only observed when both the particles and the substrate contain the complementary host−guest recognition motif. The specificity is large enough to direct the nanoparticle assembly onto targeted surface areas by prepatterning the substrate with the multivalent guest. Such a methodology may find application in nanofabrication schemes for the creation of 2D patterns of nanoparticles which can have interesting sensoric, photonic, and electronic applications.

Acknowledgment. This research was supported by the Technology Foundation STW, applied science division of NWO, and the technology program of the Ministry of Economic Affairs (Simon Stevin Nanolithography Award to D.N.R., project number TST-4946: V. M., M. P.) and

(52) We did not employ the G1 dendrimer for the surface assembly because this one can be rinsed off (see ref 37). Analogously, it has been shown for the intrinsically weaker binding, ferrocene-terminated dendrimers that G1 interacts reversibly with CD SAMs using two host−guest interactions, while G5 binds irreversibly using seven interactions (see ref 50).

(53) Xia, Y.; Whitesides, G. M. *Angew. Chem., Int. Ed.* **1998**, *37*, 550.

the MESA+ Institute for Nanotechnology (MiCS program: S. O.). The partial support of the EC-funded project NaPa (contract no. NMP4-CT-2003-500120) is gratefully acknowledged. The content of this work is the sole responsibility of the authors. We thank Christian A. Nijhuis and Dr. Alart Mulder for the synthesis of the adamantyl-terminated dendrimers and the CD heptamine, respectively.

LA047982W